ADVANCED MATERIALS

Reprint

(**1c**): $^1$H-NMR (200 MHz, $CDCl_3$) ($\delta$): 3.95 (s, 3H), 6.15 (d, $J$ = 4.1 Hz, 1H), 6.85 (d, $J$ = 4.04 Hz, 1H), 7.03 (d, $J$ = 9.22 Hz, 2H), 7.81 (s, 2H), 8.16 (d, $J$ = 9.24 Hz, 2H).

(**2b**): $^1$H-NMR (200 MHz, $CDCl_3$) ($\delta$): 2.40 (s, 3H), 6.10 (dd, $J$ = 0.9 Hz, $J$ = 3.28 Hz, 1H), 6.56 (d, $J$ = 3.24 Hz, 1H), 7.10 (d, $J$ = 9.2 Hz, 2H), 7.62 (s, 1H), 8.02 (bs, 1H), 8.17 (d, $J$ = 9.24 Hz, 2H).

(**2c**): $^1$H-NMR (200 MHz, $CDCl_3$) ($\delta$): 2.52 (s, 3H), 6.71 (dd, $J$ = 1.1 Hz, $J$ = 3.58 Hz, 1H), 6.99 (d, $J$ = 3.54 Hz, 1H), 7.06 (d, $J$ = 9.22 Hz, 2H), 7.26 (s, 2H), 7.89 (bs, 1H), 8.17 (d, $J$ = 9.22 Hz, 2H).

(**3b**): $^1$H-NMR (200 MHz, $CDCl_3$) ($\delta$): 3.80 (s, 3H), 6.78 (d, $J$ = 3.92 Hz, 1H), 6.88 (d, $J$ = 9 Hz, 2H), 7.09 (d, $J$ = 9.1 Hz, 2H), 7.40 (d, $J$ = 3.94 Hz, 1H), 7.52 (s, 1H), 8.06 (bs, 1H).

(**4b**): $^1$H-NMR (200 MHz, $CDCl_3$) ($\delta$): 2.31 (s, 3H), 6.81 (d, $J$ = 3.92 Hz, 1H), 7.05-7.14 (m, 4H), 7.40 (d, $J$ = 3.9 Hz, 1H), 7.53 (s, 1H), 8.13 (bs, 1H).

(**5a**): $^1$H-NMR (200 MHz, $CDCl_3$) ($\delta$): 3.79 (s, 3H), 6.65 (d, $J$ = 15.96 Hz, 1H), 6.86 (d, $J$ = 9.04 Hz, 2H), 7.02 (d, $J$ = 8.98 Hz, 2H), 7.16 (dd, $J$ = 9.12 Hz, $J$ = 15.94 Hz, 1H), 7.49–7.56 (m, 3H), 7.78 (bs, 1H), 8.19 (d, $J$ = 8.88 Hz, 2H).

(**5b**): $^1$H-NMR (200 MHz, $CDCl_3$) ($\delta$): 3.79 (s, 3H), 6.41 (d, $J$ = 15.81 Hz, 1H), 6.50 (d, $J$ = 3.87 Hz, 1H), 6.86 (d, $J$ = 9 Hz, 2H), 7.02 (d, $J$ = 9 Hz, 2H), 7.24 (dd, $J$ = 9.35 Hz, $J$ = 15.87 Hz, 1H), 7.34 (d, $J$ = 3.81 Hz, 1H), 7.44 (d, $J$ = 9.54 Hz, 1H), 7.79 (bs, 1H).

(**5c**): $^1$H-NMR (200 MHz, $CDCl_3$) ($\delta$): 3.79 (s, 3H), 6.63 (d, $J$ = 15.88 Hz, 1H), 6.84–7.08 (m, 5H), 7.42 (d, $J$ = 8.66 Hz, 1H), 7.81 (d, $J$ = 4.32, 1H).

(**6a**): $^1$H-NMR (200 MHz, $CDCl_3$) ($\delta$): 2.30 (s, 3H), 6.66 (d, $J$ = 15.96 Hz, 1H), 6.97 (d, $J$ = 8.52 Hz, 2H), 7.10 (d, $J$ = 8.28 Hz, 2H), 7.16 (dd, $J$ = 9.12 Hz, $J$ = 15.96 Hz, 1H), 7.52 (d, $J$ = 9.14 Hz, 1H), 7.54 (d, $J$ = 8.9 Hz, 2H), 7.75 (bs, 1H), 8.19 (d, $J$ = 8.89 Hz, 2H).

(**6b**): $^1$H-NMR (200 MHz, $CDCl_3$) ($\delta$): 2.29 (s, 3H), 6.42 (d, $J$ = 15.84 Hz, 1H), 6.50 (d, $J$ = 3.81 Hz, 1H), 6.97 (d, $J$ = 8.41 Hz, 2H), 7.09 (d, $J$ = 8.22 Hz, 2H), 7.23 (dd, $J$ = 9.38 Hz, $J$ = 15.84 Hz, 1H), 7.33 (d, $J$ = 3.87 Hz, 1H), 7.44 (d, $J$ = 9.57 Hz, 1H), 7.84 (bs, 1H).

(**6c**): $^1$H-NMR (200 MHz, $CDCl_3$) ($\delta$): 2.30 (s, 3H), 6.65 (d, $J$ = 15.72 Hz, 1H), 6.93-7.12 (m, 6H), 7.43 (d, $J$ = 9.1 Hz, 1H), 7.82 (d, $J$ = 4.32, 1H).

All the compounds were recrystallized from either methanol or acetonitrile before being used. All the physical measurements were performed in 1,4-dioxane. For details of the experimental EFISH set-up see [11]. The fundamental wavelength, $\lambda$ = 1.907 μm generated by a Nd:YAG laser at 1.06 μm in a high pressure Raman hydrogen cell was used. The $\mu\beta$ values were calibrated with a reference solution of 2-methyl-4-nitroaniline (MNA). The molecular hyperpolarizability $\beta$ of MNA was taken as $32 \times 10^{-40}$ m$^4$V$^{-1}$ as determined by an EFISH experiment with crystalline quartz ($d_{11}$ = 0.4 pm V) as a reference [11].

The ground-state dipole moment $\mu$ was derived from concentration-dependent measurements of the dielectric constant and the use of the Guggenheim equation [10].

Received: November 27, 1995
Final version: January 26, 1996

[1] For recent reviews see: C. Bosshard, K. Sutter, P. Prêtre, J. Hulliger, M. Flörsheimer, P. Kaatz, P. Günter, *Organic Nonlinear Optical Materials*, Gordon and Breach, Amsterdam **1995**. J. Zyss, *Molecular Nonlinear Optics: Materials, Physics, Devices*, Academic Press, Boston, MA **1994**. *Optical Non-linearities in Chemistry* (Ed: D. M. Burland), *Chem. Rev.* **1994**, *94*, No. 1.

[2] D. J. Williams, *Angew. Chem., Int. Ed. Engl.* **1984**, *23*, 690.

[3] L. T. Cheng, W. Tam, S. H. Stevenson, G. R. Meredith, G. Rikken, S. R. Marder, *J. Phys. Chem.* **1991**, *95*, 10631.

[4] L. T. Cheng, W. Tam, S. R. Marder, A. E. Stiegman, G. Rikken, C. W. Spangler, *J. Phys. Chem.* **1991**, *95*, 10643.

[5] F. Würthner, F. Effenberger, R. Wortmann, P. Krämer, *Chem. Phys.* **1993**, *173*, 305.

[6] A. K. Y. Jen, V. P. Rao, K. Y. Wong, J. K. Drost, *J. Chem. Soc. Chem. Commun.* **1993**, 90.

[7] R. Taylor, in *Heterocyclic Compounds – Thiophene and Its Derivatives, Vol. 44, Part 2* (Ed: S. Gronowitz), Wiley Interscience, New York **1986**, pp. 1–117.

[8] C. Bosshard, G. Knöpfle, K. Sutter, P. Günter, *Proc. SPIE* **1994**, *2143*, 187.

[9] C. Serbutoviez, C. Bosshard, G. Knöpfle, P. Wyss, P. Prêtre, P. Günter, K. Schenk, E. Solari, G. Chapuis, *Chem. Mater.* **1995**, *7*, 1198. Note that the reference value for MNA was misquoted. As in this work here, the value used there was $\beta = 32 \times 10^{-40}$ m$^4$V$^{-1}$.

[10] E. A. Guggenheim, *Trans. Faraday Soc.* **1949**, *45*, 714.

[11] C. Bosshard, G. Knöpfle, P. Prêtre, P. Günter, *J. Appl. Phys.* **1992**, *71*, 1594.

[12] B. F. Levine, C. G. Bethea, *J. Phys. Chem.* **1975**, *63*, 2666.

[13] S. K. Kurtz, T. T. Perry, *J. Appl. Phys.* **1968**, *39*, 3798.

[14] **4c** exhibits an SHG signal comparable to DANPH, as was previously reported in [9].

[15] Of the 23 type-I 4-nitrophenylhydrazone derivatives that have already been synthesized in our laboratory, 16 are SHG active.

[16] Crystal data for $C_{12}H_{11}N_3O_2S_2$: orthorhombic, $Pca2_1$: $a$ = 26.978(9), $b$ = 6.592(2), $c$ = 7.886(3) Å, $V$ = 1402.4(8) Å$^3$, $Z$ = 4, $\rho_{calcd}$ = 1.389 mg cm$^{-3}$, $T$ = 293 K. Syntex P21 diffractometer (MoKα, $\lambda$ = 0.71073 Å), 1128 measured reflections within $3 < 2\theta < 45°$, of which 998 are independent, 765 with $F > 4.0\sigma(F)$. The structure was solved by directed methods and all heavy atoms were refined by full matrix least squares procedures with 180 parameters. All H atoms were located according to the riding model with fixed isotropic $U$. $R$ = 0.0294, $wR$ = 0.0396, $w^{-1} = \sigma^2(F) + 0.0022F^2$, GOF = 0.73. Residual electron density 0.20(0.14) eÅ$^{-3}$.

[17] The dipole moment orientation in which the geometry is adapted from the crystallographic result is obtained by semi-empirical calculations using AM1 parameters in MOPAC 6.

[18] Based on the semi-empirical calculations using AM1 parameters in MOPAC 6, the difference in the heat of formation for the optimized geometry of conformers is only a few kcal mol$^{-1}$.

[19] J. Olivard, J. P. Heotis, *J. Org. Chem.* **1968**, *33*, 2552.

[20] G. Kossmehl, B. Bohn, *Chem. Ber.* **1974**, *107*, 710.

[21] B. S. Furniss, A. J. Hannaford, P. W. G. Smith, A. R. Tatchell, *Vogel's Text Book of Practical Organic Chemistry*, Wiley, New York **1989**.

## Fabrication of Single-Mode Polymeric Waveguides Using Micromolding in Capillaries**

By *Xiao-Mei Zhao, Alison Stoddart, Stephen P. Smith, Enoch Kim, Younan Xia, Mara Prentiss,** and *George M. Whitesides**

This paper describes the use of a new technique for microfabrication of polymeric structures—micromolding in capillaries (MIMIC)[1]—to make arrays of single-mode polymeric waveguides. In MIMIC, the microstructures are formed by generating a network of capillaries by contacting an elastomeric "stamp" having a relief structure on its face with a planar or curved substrate, and then allowing a liquid prepolymer to fill this network by capillary action. The elastomer we most commonly use for the stamp is

[*] Prof. G. M. Whitesides, X.-M. Zhao, E. Kim, Y. Xia
Department of Chemistry, Harvard University
12 Oxford Street, Cambridge, MA 02138-2902 (USA)
Prof. M. Prentiss, A. Stoddart
Department of Physics
Harvard University
Cambridge, MA 02138 (USA)
Dr. S. P. Smith
Research Laboratory Electronics
Massachusetts Institute of Technology
Cambridge, MA 02139 (USA)

[**] This work was supported in part by the National Science Foundation (PHY 9312572) and the Office of Naval Research and the Advanced Research Projects Agency. This work made use of MRSEC Shared Facilities supported by the National Science Foundation under Award Number DMR-9400396. The authors would like to thank Mr. Yuanchang Lu and Mr. Stephen Shepard for their assistance in using these facilities.

ADVANCED MATERIALS

polydimethylsiloxane (PDMS); it is transparent, and has a low solid-vapor interfacial free energy. The liquid prepolymer can be cured to a solid in situ by irradiation of the system with UV light. The elastomeric stamp is then peeled away, leaving the waveguide structures; adhesion between the stamp and the polymeric microstructures is not a problem for correctly chosen polymers.

Many methods[2,3] have been used to fabricate polymeric waveguides: examples include reactive ion etching,[4] UV laser[5] and e-beam[6] writing, induced dopant diffusion during polymerization (photolocking[7] and selective polymerization[8]), selective poling of electro-optically active molecules induced by an electric field,[9] and polymerization of self-assembled prepolymers.[10] MIMIC has characteristics that may give it advantages over these processes in certain applications. First, using masters (relief structures having the same shapes as the desired waveguides) made in a photolithographic process and elastomeric "stamps" complementary to these shapes, MIMIC can easily generate polymeric waveguides of different shapes and sizes; the flexibility of this procedure makes it a candidate for the fabrication of low-cost integrated optical devices with complicated structures. Second, MIMIC allows the fabrication of large numbers of waveguides in a single step. This parallelism also has the potential to produce low-cost devices. Third, MIMIC is capable of producing waveguides and claddings using a wide range of UV-curable polymers. These starting materials can be pure compounds, blends of multifunctional molecules, and polymers doped with materials such as dyes that modify optical and physical properties. The optical properties of the waveguides and the claddings can thus be changed independently over wide ranges to tune the waveguide structures for particular wavelengths and applications. Fourth, MIMIC can be used to fabricate polymeric waveguides on virtually any optically flat surface to which the polymers of the waveguides and cladding have good adhesion: it is a room-temperature process that proceeds under mild conditions. MIMIC can be used with non-planar surfaces, where projection lithographic procedures fail. Fifth, since it is a replication procedure, MIMIC can also fabricate structures in which the thickness of the waveguide differs at different points, or certain types of 3-D structures.[1]

Figure 1 outlines the procedure used to fabricate waveguides using MIMIC. The procedure has three stages. First (Figure 1a–d), the waveguides were fabricated on a silicon wafer by MIMIC. The ends of the structure were prepared by cleaving the wafer. Second (Fig. 1e–f), the cladding layer was fabricated by placing a drop of liquid prepolymer on the waveguides, and pressing a second textured stamp into this liquid. The polymer was photopolymerized, and the stamp was removed. The amount of liquid polymer applied was just enough to wet the interface between the stamp and the waveguide arrays. Using a low-viscosity (< 100 cP, 25 °C) prepolymer, we were able to keep the thickness of the cladding layer $\leq 10$ $\mu$m. Third (Fig. 1f–g), one end (the output end) of the system was again squared by fracturing the wafer substrate.

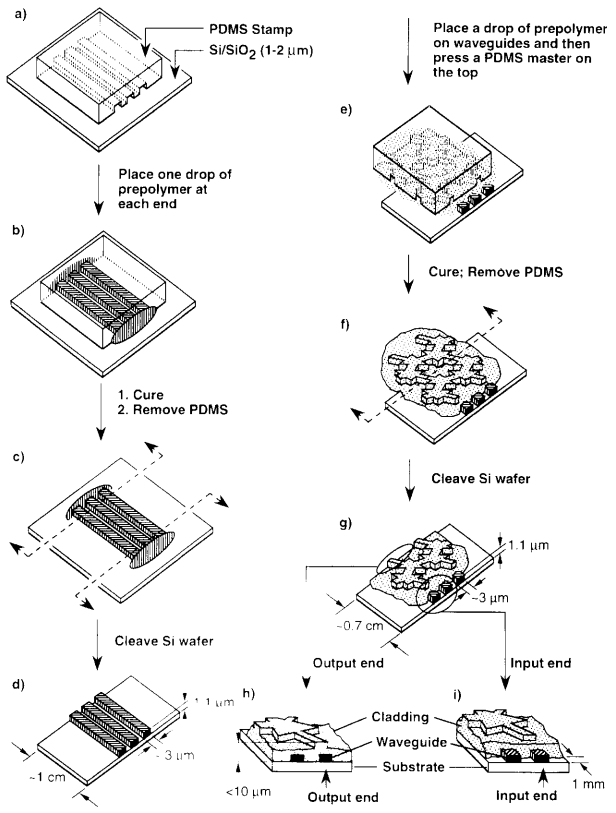


Fig. 1. Diagram outlining the fabrication of rectangular, clad channel waveguides using MIMIC.

Figure 2 shows the structures and sizes of the clad waveguides. The single-mode waveguides were sandwiched between a cladding layer and a substrate (a silicon wafer covered with a 1–2 $\mu$m thick layer of thermal silicon dioxide). The material of the waveguides had an index of refraction ($n_{guide} = 1.545$) that was slightly higher than the

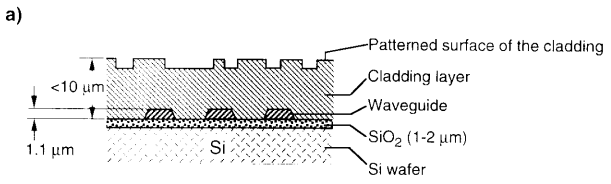


b)

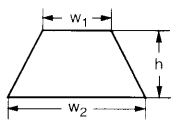


| Size | $w_1$(μm) | $w_2$(μm) | w1/w2 | h(μm) |
|---|---|---|---|---|
| A | 1.3 | 2.0 | 0.65 | 1.1 |
| B | 1.6 | 2.4 | 0.67 | 1.1 |
| C | 2.1 | 3.0 | 0.70 | 1.1 |
| D | 3.0 | 4.0 | 0.75 | 1.1 |

Fig. 2. a) A schematic of cross-sections of clad waveguides fabricated on a Si/$SiO_2$ substrate. b) The actual dimensions of the waveguides fabricated using MIMIC. There are four different sizes, size A, B, C, and D, of the waveguides mentioned in the paper. The sizes of the waveguides were measured under a scanning electron microscope (SEM).

  0935-9648/96/0505-0421 $ 10.00+.25/0 

index of the cladding layer ($n_{cladding} = 1.52–1.53$). Figure 3 shows SEM images of the clad waveguides. The cross-section of the polymeric waveguides was trapezoidal because the lines of polymer on the photoresist master that we used to make the PDMS stamps also had a trapezoidal shape. The roughness of the edges of the waveguides, shown in Figure 3c, originated in the defects of the photoresist master. The roughness may cause loss of the light.

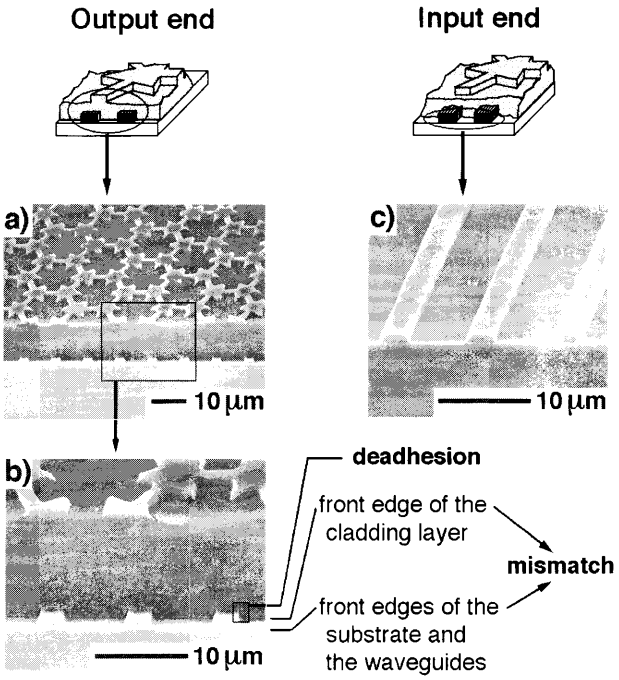


Fig. 3. SEM images of output (a and b) and input ends (c) of clad waveguides. The waveguides shown in this figure are made of polyurethane (J-91), and the cladding material is UV-cured polyacrylates (UV15-7LV). The polymeric structures were coated with ~20 nm of gold before they were examined using scanning electron microscopy.

The cladding layer started ~1 mm from one end of the network, and covered the rest of the waveguides completely (Fig. 1g–i). The unclad end was used as the input end. Since higher-order modes of the light escape from these waveguides within the first few mm of propagation, leaving ~1 mm of the waveguide open to the air made it easier to trace the optical coupling of the polymeric waveguide with the optical fiber used as a light source.

We patterned the upper surface of the cladding layer in a relief structure with feature sizes of several μm (Fig. 3). This deep, three-dimensional patterning made the cladding layer, considered as a planar, slab waveguide, extremely "lossy" and thus prevented light that was coupled into the cladding at the input end from propagating though the cladding.

Fabrication of waveguides using MIMIC required the use of UV-curable prepolymers that had relatively low viscosity (< 300 cP at 25 °C). The low viscosity allowed the capillaries (with lengths of ~1 cm) to fill completely in a reasonable amount of time (< 12 hours for a viscosity of < 300 cP). Heat-curable polymers generally are not suitable unless they remain in the liquid phase before they fully fill in the channels. We prepared the ends of the waveguides by cleaving the substrate. The polymers and the $Si/SiO_2$ wafer have very different mechanical properties; the polymeric structures and the wafer substrate may de-adhere and/or break along different fracture planes under the external mechanical stress. The problem can be addressed by reducing the thickness of the polymeric structures. In our experience, the end of the waveguides and that of the Si $SiO_2$ substrate adhered and matched well (as in Fig. 3b). The cladding was, however, much thicker than the waveguides, and differences in the geometry of the fracture surfaces in the Si $SiO_2$ layer and the cladding layer often resulted in an offset in the ends of these structures.

At the current stage of development of this technique for fabrication, we were not able to obtain the well-ordered structures shown for the exit region of the clad waveguide (Fig. 1h) consistently. A little de-adhesion and a mismatch of less than 1 μm between the end of the cladding layer and the end of the waveguides (Fig. 3b) did not, however, seem to distort the pattern of light exiting the waveguide.

Light from a laser was coupled into a waveguide by butting[10] an optical fiber against its end. We have demonstrated guiding for light with wavelengths = 0.55 μm (He–Ne laser), 0.63 μm (He–Ne laser), and 0.85 μm (diode laser); these wavelengths correspond to core diameters of 3.1 μm, 4.0 μm, and 5.5 μm in the fibers respectively. Unclad waveguides (J-91, polyurethane, $n_{guide} = 1.545$) with cross-sections of ~3 $\mu m^2$ (Fig. 2) support multiple modes with light having wavelengths = 0.55–0.85 μm.

Clad waveguides, fabricated as described, could be either single-mode or multi-mode depending on the size of the waveguides, the wavelength of the light, and the refractive indices of the materials of which waveguides and claddings were fabricated. Figure 4a shows a second-order mode for 0.55 μm light in a size-D (Fig. 2) J-91 waveguide ($n_{guide}$ = 1.545) with a UV11-3 cladding (multifunctional polyacrylates, $n_{cladding}$ = 1.52), where at least three modes were allowed. For waveguides with smaller cross-sections, fewer modes were allowed to propagate. A J-91 waveguide of size A with a UV11-3 cladding allowed only two modes for 0.55 μm light.

The number of modes can also be decreased by increasing the wavelength of the light since the determining parameter is the ratio of the size of the waveguide to the optical wavelength. A clad waveguide (J-91 clad with UV11-3, $n_{guide}$ = 1.545, $n_{cladding}$ = 1.52) of size A, which allowed two modes for 0.55 μm light, transmitted only the single lowest-order mode for 0.85 μm light (Fig. 4b). This performance can be compared with the single allowed propagating mode (Fig. 4c) for 0.85 μm light in the optical fiber of a 5.5 μm diameter which was used to couple into the waveguide.

As expected, decreasing the size of the waveguides and increasing the wavelength of the light decreased the number of the modes allowed to propagate. Decreasing the index difference between the cladding and the waveguides also decreased the number of allowed modes. Waveguides (J-91,


© VCH Verlagsgesellschaft mbH, D-69469 Weinheim, 1996 0935-9648/96/0505-0422 $ 10.00+.25/0 Adv. Mater. 1996, 8, No. 5

ADVANCED MATERIALS

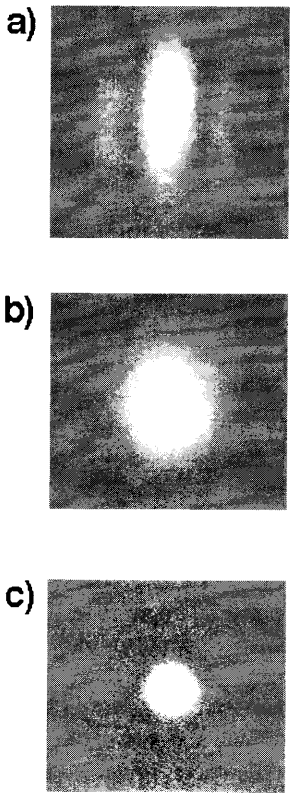


Fig. 4. Photographs of a) the multi-mode output from a clad waveguide (J-91 clad with UV11-3) of size D using 0.55 $\mu$m light, b) the single-mode output from a smaller clad waveguide (J-91 clad with UV11-3, size A) using 0.85 $\mu$m light, and c) the output of 0.85 $\mu$m laser light from a single-mode optical fiber (core diameter = 5.5 $\mu$m) recorded by a CCD camera at same distance as the output end of the waveguide used in b). This output from the optical fiber was used as the input source for the clad waveguide in b). The smaller mode size in c) compared with that in b) indicates that the area of the core of this input fiber was bigger than the cross-sectional area of the waveguide in b).

$n_{guide}$ = 1.545) of sizes A and B were single-mode at a wavelength of 0.55 $\mu$m when they were clad with UV15-7LV (multifunctional polyacrylates, $n_{cladding}$ = 1.53), whereas the same waveguides clad with UV11-3 ($n_{cladding}$ = 1.52) allowed two modes to propagate. For a cladding of UV15-7LV on these waveguides, two modes were not allowed to propagate until the cross-section was of size C.

All these observations, except the shapes of modes, were consistent with the theoretical calculations.[11] The modes were more symmetric than the results of the calculations, i.e., the ratio of the height to the width of a mode was smaller than the ratio obtained from the calculation. We hypothesize that there may have been an index gradient across the face of each waveguide due to the differential mechanical stress in the process of cleavage. The resulting lens at the output end of the waveguide would change the shapes of output modes.

Since the areas of the cores of the cylindrical optical fibers were larger than the cross-sectional areas of the trapezoidal polymeric waveguides, the efficiency of butt coupling from a fiber into a polymeric waveguide was low. The measured ratio of the intensity at the output of a single-mode waveguide (0.7 cm long, J-91 clad with UV11-3, size A, 0.85 $\mu$m light, fiber core diameter = 5.5 $\mu$m) to the intensity at the fiber output ranged between 0.05 and 0.10. The efficiency of transmission and coupling were independent of the polarization of the incoming light. When the waveguides were fabricated on a gold substrate, the intensity of the output was strongly dependent on the polarization of the input, and the output was strongly linearly polarized with the electric field parallel to the substrate.

We have also coupled light into an unclad waveguide saturated with rhodamine 590 chloride. Light ($\lambda$ = 0.488 $\mu$m, blue) propagating in the waveguide excited the molecules of the dopant; the resulting fluorescence (green) lit up the entire waveguide.

Fabrication of waveguides using MIMIC still has several limitations. First, the preparation of the ends of the waveguides by fracturing is not entirely reproducible. The de-adhesion and mismatch at the output end can, sometimes, distort the pattern of the exciting light. Fabricating reproducible and optically optimized ends is a technical challenge remaining to be solved. Second, the properties and/or dimensions of the polymers may change on cross-linking, irradiation or heating. Third, the rate of filling of the capillaries is slow and inversely proportional to the length of the channel that the liquid travels.[11] Fabrication of a waveguide with length ~1 cm requires several hours, and the maximum length of the channel to be filled by a liquid prepolymer (~300 cP) at 25 °C is 1.5 cm.

Despite these limitations, micromolding in capillaries provides a new, low-cost, simple method to fabricate single-mode polymeric waveguides. This procedure is straightforward operationally. The ease with which MIMIC generates complex polymeric microstructures with $\mu$m-scale dimensions, its ability to fabricate a range of classes of materials, and its ability to generate complex topologies and to accept non-planar surfaces as substrates, all provide capabilities that can be applied to the fabrication of waveguides.

## *Experimental*

The unclad waveguides were prepared by MIMIC, using a master made from poly(dimethylsiloxane) (PDMS, Sylgard 184, Dow Corning, Silicone Elastomer: its curing agent = 20:1) as described previously [1]. The supporting surface was a silicon(100) wafer covered with 1–2 $\mu$m thick layer of thermal silicon dioxide (Silicon Sense, Inc.). The top surface of the unclad waveguides were oxidized slightly in a UV ozone cleaner to improve adhesion between them and the polymeric cladding layer. A drop of liquid prepolymer of a cladding material was placed on top of the waveguides and a PDMS master was then pressed down into this drop. The prepolymer spread into a thin layer ($\leq$ 10 $\mu$m thick) between the master and the waveguides. The first ~1 mm of the network from the input end was kept away from the prepolymer of the cladding layer. The prepolymer constituting the cladding layer was cured by UV irradiation. The PDMS stamp was removed, and the output end was cleaved.

We have fabricated waveguides with UV-cured polyurethane (J-91, Summers Optical; and NOA 73, Norland), UV-cured polyacrylates (UV11-4M1, Masters), UV-cured epoxy (UV15, Master Bond, Inc.), and rhodamine-doped polyurethane (J-91 saturated with rhodamine 590 chloride, Exciton). We have clad waveguides of polyurethane (J-91) with UV-cured polyacrylates (UV11-3, UV11-4M1, UV15-7LV, Master Bond, Inc.).

Received: December 18, 1995

[1] E. Kim, Y. Xia, G. M. Whitesides, *Nature* **1995**, *376*, 581.
[2] L. R. Dalton, A. W. Harper, B. Wu, R. Ghosn, J. Laquindanum, Z. Liang, A. Hubbel, C. Xu, *Adv. Mater.* **1995**, *7*, 519.
[3] B. L. Booth, *J. Lightwave Technol.* **1989**, *7*, 1445.
[4] M. Kagami, H. Ito, T. Ichikawa, S. Kato, M. Matsuda, N. Takahashi, *Appl. Opt.* **1995**, *34*, 1041.
[5] A. Mukherjee, B. J. Eapen, S. K. Baral, *Appl. Phys. Lett.* **1994**, *65*, 3179.
[6] M. J. Rooks, H. V. Roussell, L. M. Johnson, *Appl. Opt.* **1990**, *29*, 3880.
[7] E. A. Chandross, C. A. Pryde, W. J. Tomlinson, H. P. Weber, *Appl. Phys. Lett.* **1974**, *24*, 72.
[8] T. Kurokawa, N. Takato, Y. Katayama, *Appl. Opt.* **1980**, *19*, *18*, 3124.
[9] J. I. Thackara, G. F. Lipscomb, M. A. Stiller, A. J. Ticknor, R. Lytel, *Appl. Phys. Lett.* **1988**, *52*, 1031.
[10] E. Kim, G. M. Whitesides, L. K. Lee, S. P. Smith, M. Prentiss, *Adv. Mater.* **1996**, *8*, 139.
[11] *Guided-Wave Optoelectronics* (Ed: T. Tamir) 2nd ed., Springer-Verlag, New York **1990**.

## Oxygen Ion Conductivity of Platinum-Impregnated Stabilized Zirconia in Bulk and Microporous Materials**

By *Andreas Ziehfreund, Ulrich Simon,* and *Wilhelm F. Maier**

Yttria stabilized zirconia (YSZ) is a well known solid electrolyte with good oxygen ion conductivity at high operating temperatures (> 500 °C). Thin films made from this material are of great interest, especially for the manufacturing of catalytic membrane reactors,[1] solid oxide fuel cells,[2] electrochemical oxygen sensors[3] or the production of oxygen semipermeable membranes. Major problems of present oxygen conductors are the high operating temperature and the rather low permeability. For practical applications, materials with significantly lower operating temperature and higher permeability are needed.

Oxygen ion transport through the bulk is a materials property, while the oxygen transfer from the gas phase into the solid and back should depend on available surface area and activation barriers. Increase of surface area by the use of highly porous material and reduction of the activation barrier for chemisorption are modifications which may improve the oxygen ion conductivity. The oxygen transport properties of solid electrolyte membranes are affected by catalytic activation of oxygen on the surface. According to Pizzini[4] platinum electrodes on the surface of solid electrolytes enhance the oxygen exchange rate of the material by influencing the oxygen adsorption equilibrium at the electrolyte surface, promoting the overall charge transfer reaction at the three phase contact gas/electrode/electrolyte (Eq. 1).

$$1/2\ O_2(\text{gas}) + 2e^-(\text{electrode}) \rightleftharpoons O^{2-}(\text{electrolyte}) \qquad (1)$$

Thin films of microporous metal oxides with a narrow pore size distribution and a large surface area can be prepared conveniently by electron beam evaporation.[5] We expected that microporous thin-film solid electrolyte materials with a large inner surface with incorporated highly dispersed platinum particles, accessible to the gas phase, would allow a higher oxygen reaction rate and thus enhance oxygen ion conductivities, especially at lower temperatures. Because microstructural variations are known to have an enormous effect on the ionic conductivities of zirconia electrolytes[4,6] these thin film materials might exhibit new electrochemical transport properties. These properties will need to be characterized before potential applications of the thin films, for example in oxygen-selective membranes can be considered.

In this communication we report the preparation and a study of the ionic conductivity of bulk and microporous Pt-stabilized zirconia. The materials were investigated by complex impedance spectroscopy in the temperature range 200–600 °C in an oxygen atmosphere. This method is an excellent tool for the study of the microstructural properties of YSZ phases and provides the possibility to distinguish between bulk, grain boundary and electrode polarization effects for various kinds of ionic conductors.[7,8]

Bulk YSZ (9.1 mol % $Y_2O_3$) was prepared from powders from aqueous slurries by standard sintering methods, parts were impregnated with Pt (1 wt.-% Pt). The pelleted samples were evaporated by an e-beam and condensed on aluminum foil, resulting in a microporous thin film. The thin film material was isolated by dissolving the aluminum foil in aqueous acid,[5] filtered, dried and powdered (microporous samples). The chemical composition of the bulk and microporous samples was confirmed by XFS and AAS. The Pt content in the microporous YSZ increased to 1.5 wt.-%. The negligible enrichment from 9.1 to 9.3 mol % $Y_2O_3$ in the microporous materials should have no effect on the ionic conductivity, which for the system YSZ is nearly constant in the composition range 6–12 mol % $Y_2O_3$.[9] The enrichment of Pt and $Y_2O_3$ can be explained by the variation in evaporation rates, which decrease in the order $Pt > Y_2O_3 > ZrO_2$. The Pt content in both is far below the percolation threshold so that electronic conductivity in parallel to the ionic charge transport can be ruled out.[10]

X-ray powder diffraction patterns show the presence of the cubic structure of YSZ in the bulk as well as in the microporous system. The microporous material exhibits only slight peak broadening. Nitrogen sorption isotherms (BET) showed no measurable surface area of the highly sintered and compact bulk samples (< 1 $m^2/g$), while the

[*] Prof. W. F. Maier, Dr. A. Ziehfreund
Max-Planck-Institut für Kohlenforschung
Kaiser-Wilhelm-Platz 1, D-45470 Mülheim a. d. Ruhr (Germany)
Dr. U. Simon
Institut für Anorganische Chemie
Universität Essen
Schützenbahn 70, D-45127 Essen (Germany)

[**] We wish to thank Prof. G. Schön for access to his impedance spectrometer, Dr. H. Wiggers for the performance of measurements, and the BMFT, grant No. 03C257B, for financial support.



0935-9648/96/0505-0424 $ 10.00+.25/0